

## Charge transfer in alkali-metal-doped polymeric fullerenes

J. Winter and H. Kuzmany

*Institut für Materialphysik, Universität Wien Strudlhofgasse 4, A-1090 Wien, Austria*

A. Soldatov, P.-A. Persson, P. Jacobsson, and B. Sundqvist

*Department of Experimental Physics, Umeå University, S-901 87 Umeå, Sweden*

(Received 29 July 1996)

We present room-temperature Raman measurements of pressure-polymerized  $C_{60}$  and compare them with the spectra of  $RbC_{60}$  in the orthorhombic phase. Although both materials were prepared according to two completely different routes the spectra show a surprising similarity with respect to mode positions and line splitting. We concluded from this that both materials, the uncharged pressure-polymerized  $C_{60}$  and the rubidium-doped orthorhombic compound, have the same overall structure and the  $AC_{60}$  compounds can be considered as the doped species of the  $C_{60}$ , polymerized using moderate low pressure and high temperatures. From a detailed comparison between both spectra mode shifting and line broadening as a consequence of the charge transfer was determined and electron-phonon coupling constants were estimated for the high-frequency  $H_g(7)$  and  $H_g(8)$  modes. The low values for the coupling constants compared to the ones in the  $K_3C_{60}$  can explain the lack of superconductivity in the  $AC_{60}$  compounds. [S0163-1829(96)06448-X]

### I. INTRODUCTION

In the last few years considerable experimental and theoretical research has been dedicated to the various forms of polymeric fullerenes. The first member of this new family of materials was phototransformed  $C_{60}$ . The photosensitivity of  $C_{60}$  was already noticed in the early days of fullerene research since Raman spectra obtained for very clean material at room temperature were found to be unstable if the energy of the exciting laser was larger than about 1.8 eV. Arguments for the description of the photoproduct as a polymer came from its insolubility and from characteristic mass spectra which were quite different before and after irradiation of  $C_{60}$  with appropriate light. A suggestion to explain the transformation process came from Rao *et al.*<sup>1</sup> in the form of a  $2 + 2$  cycloaddition after the absorbed laser light had induced a highly reactive triplet state on the  $C_{60}$  molecule. The  $2 + 2$  cycloaddition process has since then been considered as the basic mechanism for polymerization in  $C_{60}$ .

More or less simultaneously with the observation of the phototransformation the phases  $AC_{60}$  were discovered<sup>2-4</sup> for  $A = K$  and  $Rb$  and later also for  $Cs$ . The phases have a rocksalt structure at high temperatures and are subjected to a phase transition on cooling either to an orthorhombic state ( $Rb$ ,  $Cs$ ) or for  $K$ , if the cooling speed is low enough, to a phase-separated compound  $\alpha-C_{60} + K_3C_{60}$ . If the cooling rate for the potassium compound is fast enough the same phase as for the  $Rb$  and  $Cs$  compound is obtained. For the orthorhombic structure an unusual low distance of 9.2 Å was observed between two molecules along a (110) direction from which a polymeric character for the compounds was deduced.<sup>5</sup> In contrast to the thin films of phototransformed material an extended structural study with Rietveld refinement was possible. The latter resulted in reliable values for the bond lengths between the connected molecules.<sup>6</sup>

In the polymeric state  $AC_{60}$  has several remarkable properties, such as a metallic character of the electronic system,<sup>7</sup>

stability versus ambient conditions,<sup>8</sup> and at least for the  $Rb$  and  $Cs$  compound a magnetic phase transition to an insulating state.<sup>9</sup>  $KC_{60}$  remains metallic to low temperatures but does not become superconducting.

Finally, reacted compounds of  $C_{60}$  were most recently observed also after treatment of the material at elevated temperature and high pressure.<sup>10,11</sup> The observed structures depended strongly on the pressure and temperatures used in the experiments. After rapid compression of  $C_{60}$  up to 20 GPa at room temperature and under nonhydrostatic conditions polycrystalline bulk diamond could be obtained.<sup>12</sup> X-ray analysis indicates a fcc lattice with a diamond structure. Quasihydrostatic pressures  $> 18$  GPa together with a large shear deformation lead to a new form of amorphous carbon which is harder than diamond but may still be related to  $C_{60}$ .<sup>13</sup>

In contrast, if quasihydrostatic pressures of about 5 GPa were used, different structures were found depending on the temperature. Iwasa *et al.*<sup>10</sup> report the formation of a rhombohedral structure at 700 °C and a second phase at 300 °C which can be indexed using a distorted fcc structure. The small measured values for the intermolecular distance and the fact that the material was insoluble in toluol and converted to normal  $C_{60}$  after heating suggests a chemical bonding between the molecules. The expected symmetry reduction of linked molecules is consistent with the increasing number of observed vibrational modes in the Raman and infrared (IR) measurements.

A detailed x-ray structural analysis was done by Regueiro *et al.*<sup>11</sup> In this investigation the x-ray pattern of the phase at 700 °C could be simulated using a mixture of a majority rhombohedral and a minority tetragonal phase. For samples prepared at 8 GPa and a temperature of 300 °C the x-ray spectra are close to those of the distorted fcc phase of Iwasa *et al.* but the spectra showed additional features and could be simulated with a body-centered orthorhombic structure. So, the x-ray refinement leads to an orthorhombic structure where the molecules are suggested to be linked together by

four-membered rings forming linear chains.

Some recent results of Persson *et al.*<sup>14</sup> demonstrated a polymerization process of  $C_{60}$  between 550 and 585 K at even lower pressure of only 1.1 GPa. The x-ray measurements agree qualitatively with the orthorhombic structure of linear polymer chains found at high pressure in Ref. 11 but a more detailed analysis could not be done because of broad overlapping peaks. However, in Refs. 14 and 15 it has been demonstrated that bonding between molecules has a covalent nature: magic angle spinning NMR revealed  $sp^3$  hybridization. Recent experiments by Sundqvist *et al.*<sup>16</sup> showed that polymerization reaction starts in  $C_{60}$  already at  $p = 0.8$  GPa and 450 K.

In this paper we present detailed Raman spectra for the low-pressure-polymerized orthorhombic  $C_{60}$  and compare it with similar spectra obtained for the orthorhombic phase of doped  $AC_{60}$ . Even though the preparation of the two materials was along completely different routes the spectra showed a striking similarity not only with respect to line positions but also with respect to details of the splitting of the lines. This allowed us to establish a reliable correlation between the vibrational modes in the two materials and, consequently, the charge-transfer-generated polymer can be considered as the doped phase of the pressure-polymerized material. Thus the charge-transfer-induced line shifts and line shapes could be determined. From the difference in the linewidths an estimation of the electron-phonon coupling constants for the modes in metallic  $RbC_{60}$  was possible. These coupling constants turned out to be much smaller as compared to  $K_3C_{60}$ , which explains why neither  $KC_{60}$  nor  $RbC_{60}$  is a superconductor.

## II. EXPERIMENT

To produce the pressure-polymerized samples 99.99% pure  $C_{60}$  powder was encapsulated in a stainless steel container of a high-pressure cell and subjected initially to 0.2 GPa. Subsequently the sample was heated to a reaction temperature of about 300 °C. Then the pressure was increased to 1.1 GPa and the sample was annealed for several hours. Before the pressure was lowered to zero the sample was cooled to room temperature. After the pressure treatment the structure of the sample was analyzed by x rays. The result agreed qualitatively with an orthorhombic structure. Experimental details for the pressure treatment of the  $C_{60}$  powder are described by Soldatov *et al.*<sup>15</sup>

$RbC_{60}$  was prepared by doping  $C_{60}$  single crystals *in situ* in front of a Raman spectrometer. The doping was performed by a combination of load and equilibration processes above 410 K as described in detail by Winter and Kuzmany in Ref. 17. It was continued well beyond the disappearance of any signal from undoped  $C_{60}$  in the Raman spectrum. Thus the crystals were doped at least to the penetration depth of the laser used for the excitation of the Raman spectra. After the doping the crystals were slowly cooled to room temperature in order to obtain the orthorhombic polymeric phase.

The Raman measurements were performed at room temperature and at 450 K using an argon ion laser with an excitation of 514.5 nm. The laser power was kept to approximately 50 W/cm<sup>2</sup>. The scattered light was analyzed with a Dilor  $xy$  spectrometer and registered with a multichannel

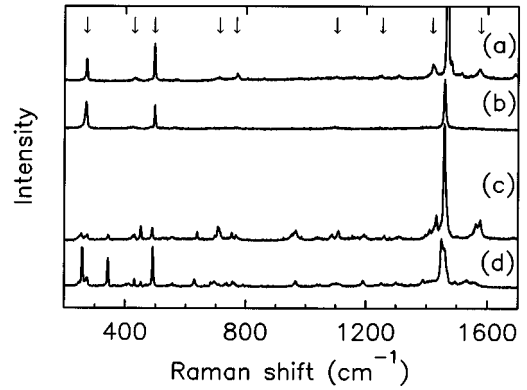


FIG. 1. Overall Raman spectra of (a)  $C_{60}$  and (b)  $RbC_{60}$ , both at 450 K. (c) and (d) are the Raman spectra of pressure-polymerized  $C_{60}$  and  $RbC_{60}$  in the orthorhombic phase at room temperature. The arrows assign the Raman active  $H_g$  modes.

charge-coupled device (CCD) detector. During the measurements the samples were kept in a vacuum better than  $10^{-4}$  Pa. The Raman data were analyzed and fitted with Voigtian line shapes using a commercial computing program. Linewidths are given as measured. The experimentally observed width of the laser was  $3 \text{ cm}^{-1}$ .

## III. RESULTS

Figure 1 shows the overall Raman spectra for  $C_{60}$  and  $RbC_{60}$  as observed at 450 K between  $200 \text{ cm}^{-1}$  and  $1700 \text{ cm}^{-1}$ , together with the pressure-polymerized orthorhombic  $C_{60}$  and the polymeric orthorhombic phase of  $RbC_{60}$  at room temperature. The spectrum of  $C_{60}$  at 450 K shows the well known  $2A_g$  modes at  $496 \text{ cm}^{-1}$  and  $1467 \text{ cm}^{-1}$  and the 8  $H_g$  modes assigned by arrows in the figure. The Raman spectrum of  $RbC_{60}$  in the rocksalt structure is similar but the pinch mode is strongly reduced in intensity and most of the  $H_g$  modes became very weak. The spectrum was discussed recently in detail for the potassium compound in Ref. 18. The downshift of the pinch mode due to the charge transfer is  $7 \text{ cm}^{-1}$ .

Figures 1(c) and 1(d) show the overall Raman spectrum for the pressure-polymerized  $C_{60}$  and for the charge-transfer-polymerized  $RbC_{60}$ . As compared to the upper two spectra several new modes can be seen together with a strong splitting of the former  $H_g$  modes. Compared with each other the spectra for the polymers exhibit a surprising similarity. Even details of line splitting look the same, as will be demonstrated explicitly in the following. The dominance of the pinch mode for the pressure-polymerized material is nearly as strong as for the pristine material. Also, this dominance has disappeared in both cases for the doped materials. For the charge-transfer-polymerized material the low-frequency part of the spectrum becomes dominant. To demonstrate the difference between the two spectra several spectral windows will be shown below with strong magnification.

Five windows of the spectrum are selected in the following. The lines in the figures mark the center positions of modes which are obtained by peak-fit analysis. These positions are listed in Table II together with the intensity and linewidth.

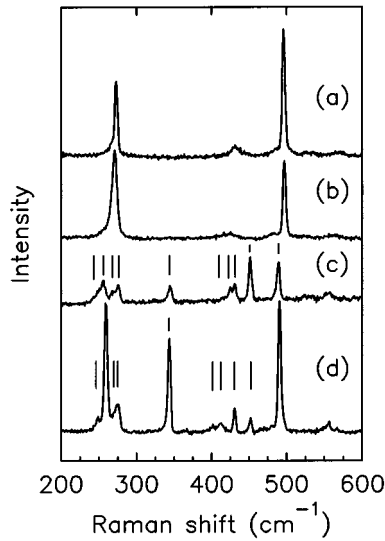


FIG. 2. Raman spectra between  $200\text{ cm}^{-1}$  and  $600\text{ cm}^{-1}$  of  $\text{C}_{60}$ ,  $\text{RbC}_{60}$  both at  $450\text{ K}$  [(a) and (b)], and pressure-polymerized  $\text{C}_{60}$  and  $\text{RbC}_{60}$  at room temperature [(c) and (d)]. The lines indicate the peak positions of the modes in the spectra.

Figure 2 shows the frequency range of the  $H_g(1)$ ,  $H_g(2)$ , and the  $A_g(1)$  mode. Even though the spectra for the polymeric phases exhibit a much richer structure a correlation to the original intrinsic Raman active modes is possible for nearly all lines. The splitting range for the  $H_g(1)$ - and  $H_g(2)$ -derived modes is  $27$  and  $36\text{ cm}^{-1}$ , if the mode at  $344\text{ cm}^{-1}$  is not included in the  $H_g(1)$ . For the doped polymer the splitting is  $26\text{ cm}^{-1}$  and  $50\text{ cm}^{-1}$ , respectively. The line shifts between neutral and charged cages on the chains are given in Table II. This table contains also the line shifts between the undoped and the single charged monomer in the ninth column. Compared to the latter the overall shift for the polymeric phases is much weaker in the case of the  $H_g(1)$  mode but similar for the  $H_g(2)$  mode. The polymerization-

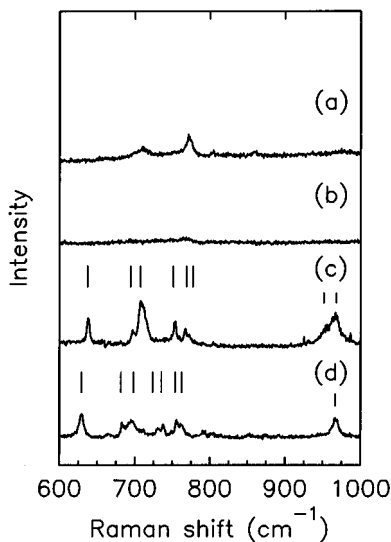


FIG. 3. Raman spectra between  $600\text{ cm}^{-1}$  and  $1000\text{ cm}^{-1}$  of  $\text{C}_{60}$ ,  $\text{RbC}_{60}$  both at  $450\text{ K}$  [(a) and (b)], and pressure-polymerized  $\text{C}_{60}$  and  $\text{RbC}_{60}$  at room temperature [(c) and (d)].

TABLE I. Correlation table of symmetry groups  $I_h$  and  $D_{2h}$ .

| $I_h$     | $D_{2h}$                              |
|-----------|---------------------------------------|
| $2A_g$    | $2A_g$                                |
| $3T_{1g}$ | $3B_{1g} + 3B_{2g} + 3B_{3g}$         |
| $4T_{2g}$ | $4B_{1g} + 4B_{2g} + 4B_{3g}$         |
| $6G_g$    | $6A_g + 6B_{1g} + 6B_{2g} + 6B_{3g}$  |
| $8H_g$    | $16A_g + 8B_{1g} + 8B_{2g} + 8B_{3g}$ |

induced shift for the  $A_g(1)$  mode is about  $7\text{ cm}^{-1}$  to lower wave numbers. On doping the line shifts upwards by  $1\text{ cm}^{-1}$  as for the monomers. It remains unsplit, as might be expected from its nondegenerate character. No direct correlation to the monomers can be found for the well expressed mode at  $344\text{ cm}^{-1}$  unless it is considered as one of the five components of the split  $H_g(1)$  mode.

Figures 3 and 4 show windows of the spectra in the range of the modes  $H_g(3)$ ,  $H_g(4)$  and  $H_g(5)$ ,  $H_g(6)$ , respectively. From both figures it is evident that even details of the split structures are retained for the two polymers. The well defined line at  $638\text{ cm}^{-1}$  is another example for a new mode not observed in the monomer phases. The assignment to the modes  $H_g(5)$  and  $H_g(6)$  is not as clear as for the other modes. However, this is already so for the relation between the pristine and the doped monomer phases. A tentative assignment to the former  $H_g$  modes is used in Table II, even for the split components.

Finally, Fig. 5 shows the frequency range of the two highest  $H_g$  modes and the pinch mode. The high-temperature spectrum for the rocksalt phase of  $\text{RbC}_{60}$  demonstrates the effect the doping has on the Raman response for the monomer and for the polymer. The lines are strongly broadened and reduced in intensity for the doped system. The behavior is similar for the doping process of the polymer except that the lines are split for both the undoped and the doped material. This similarity is particularly evident for the  $H_g$  modes

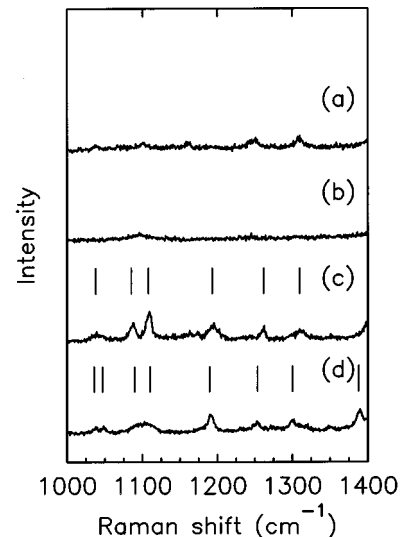


FIG. 4. Raman spectra between  $1000\text{ cm}^{-1}$  and  $1400\text{ cm}^{-1}$  of  $\text{C}_{60}$ ,  $\text{RbC}_{60}$  both at  $450\text{ K}$  [(a) and (b)], and pressure-polymerized  $\text{C}_{60}$  and  $\text{RbC}_{60}$  at room temperature [(c) and (d)].

appearing at 1423 and 1574  $\text{cm}^{-1}$  for the pristine monomer. Within experimental error the broadening and the downshift of the individual components is the same for the polymers as for the monomers. This can be seen from the quantitative results compiled in Table II.

The pinch mode for the pressure-polymerized  $\text{C}_{60}$  is downshifted by about 8  $\text{cm}^{-1}$  compared to the pristine  $\text{C}_{60}$ . The observed line can only be reproduced properly by two oscillators which were located at 1459  $\text{cm}^{-1}$  and 1464  $\text{cm}^{-1}$ , respectively. A similar splitting is observed for the pinch mode in  $\text{RbC}_{60}$  with the two components located at 1450  $\text{cm}^{-1}$  and 1460  $\text{cm}^{-1}$ . The overall shift between the undoped and the doped polymer is about the same as for the monomers.

We have also checked the frequency range of the interball

modes extending from about 70 to 200  $\text{cm}^{-1}$ . For excitation with a Nd-YAG (YAG denotes yttrium aluminum garnet) laser weak interball modes were observed at 97  $\text{cm}^{-1}$ , 119  $\text{cm}^{-1}$ , and 173  $\text{cm}^{-1}$  (Refs. 14 and 15) for the pressure-polymerized material but no equivalent modes could be observed for the green laser excitation either for the pressure-polymerized  $\text{C}_{60}$  or for the  $\text{RbC}_{60}$ .

#### IV. DISCUSSION

One reason for the dramatic changes in the Raman spectrum from the high-temperature fcc phase compared to the room-temperature orthorhombic phase is the reduction of the symmetry to  $D_{2h}$ . In  $D_{2h}$  all modes are nondegenerated and all gerade modes become Raman active. So a splitting of the

TABLE II. Positions of the Raman modes of pressure-polymerized  $\text{C}_{60}$  and polymeric  $\text{RbC}_{60}$  at room temperature.  $\Delta\omega_{\text{po}}$  and  $\Delta\omega_{\text{mo}}$  are the frequency shifts between the undoped and doped polymer and undoped and doped monomer at 450 K, respectively. The intensities are normalized to the intensity of the  $A_g(1)$  mode.

| Mode     | Pressure-polymerized $\text{C}_{60}$ |                     |                                  | Polymerized $\text{RbC}_{60}$    |                     |                                  | $\Delta\omega_{\text{po}}$<br>( $\text{cm}^{-1}$ ) | $\Delta\omega_{\text{mo}}$<br>( $\text{cm}^{-1}$ ) |
|----------|--------------------------------------|---------------------|----------------------------------|----------------------------------|---------------------|----------------------------------|--|--|
|          | $\omega$<br>( $\text{cm}^{-1}$ )     | Intensity<br>(a.u.) | $\gamma$<br>( $\text{cm}^{-1}$ ) | $\omega$<br>( $\text{cm}^{-1}$ ) | Intensity<br>(a.u.) | $\gamma$<br>( $\text{cm}^{-1}$ ) |  |  |
| $H_g(1)$ | 249                                  | 26                  | 8                                | 249                              | 9                   | 7                                | 0  |  |
|          | 256                                  | 51                  | 6                                | 259                              | 98                  | 5                                | +3   | -4   |
|          | 269                                  | 27                  | 9                                | 269                              | 10                  | 9                                | 0  | -2   |
|          | 276                                  | 38                  | 5                                | 275                              | 17                  | 6                                | -1   |  |
|          | 344                                  | 39                  | 6                                | 344                              | 71                  | 5                                | 0  |  |
| $H_g(2)$ | 416                                  | 7                   | 6                                | 402                              | 4                   | 5                                | -14  |  |
|          | 425                                  | 35                  | 5                                | 412                              | 6                   | 9                                | -13  |  |
|          | 431                                  | 41                  | 5                                | 431                              | 18                  | 5                                | 0  | -9   |
|          | 452                                  | 112                 | 5                                | 452                              | 10                  | 5                                | 0  |  |
| $A_g(1)$ | 489                                  | 100                 | 5                                | 490                              | 100                 | 5                                | +1   | +1   |
| $H_g(3)$ | 638                                  | 67                  | 5                                | 629                              | 17                  | 8                                | -9   |  |
|          | 698                                  | 33                  | 5                                | 684                              | 7                   | 5                                | -14  |  |
| $H_g(4)$ | 708                                  | 97                  | 7                                | 696                              | 12                  | 14                               | -12  |  |
|          | 754                                  | 57                  | 5                                | 731                              | 5                   | 6                                | -23  |  |
|          |                                      |                     |                                  | 738                              | 5                   | 6                                |  |  |
|          | 768                                  | 33                  | 7                                | 756                              | 10                  | 5                                | -12  | -4   |
|          | 775                                  |                     | 5                                | 762                              | 8                   | 8                                | -13  |  |
|          | 952                                  | 28                  | 14                               |                                  |                     |                                  |  |  |
| $H_g(5)$ | 967                                  | 71                  | 14                               | 967                              | 13                  | 10                               | 0  |  |
|          | 1041                                 | 13                  | 18                               | 1038                             | 4                   | 8                                | -3   |  |
|          |                                      |                     |                                  | 1049                             | 3                   | 7                                | +8   |  |
| $H_g(6)$ | 1087                                 | 39                  | 9                                | 1092                             | 5                   | 20                               | -5   | -5   |
|          | 1109                                 | 69                  | 9                                | 1109                             | 5                   | 19                               | 0  |  |
| $H_g(7)$ | 1194                                 | 39                  | 12                               | 1191                             | 14                  | 7                                | -3   |  |
|          | 1261                                 | 30                  | 8                                | 1251                             | 5                   | 9                                | -10  |  |
| $A_g(2)$ | 1310                                 | 27                  | 8                                | 1300                             | 7                   | 10                               | -10  |  |
|          | 1398                                 | 22                  | 9                                | 1389                             | 12                  | 11                               | -9   |  |
|          | 1411                                 | 60                  | 9                                | 1407                             | 7                   | 16                               | -4   | -15  |
|          | 1426                                 | 75                  | 14                               |                                  |                     |                                  |  |  |
|          | 1434                                 | 149                 | 6                                | 1424                             | 8                   | 20                               | -10  |  |
| $H_g(8)$ | 1446                                 | 59                  | 10                               |                                  |                     |                                  |  |  |
|          | 1458                                 | 878                 | 6                                | 1450                             | 94                  | 9                                | -8   | -7   |
|          | 1464                                 | 299                 | 10                               | 1460                             | 81                  | 11                               | -4   |  |
|          |                                      |                     | 1493                             | 9                                | 12                  |                                  |  |  |
| $H_g(8)$ | 1563                                 | 110                 | 18                               | 1530                             | 14                  | 34                               | -33  | -21  |
|          | 1577                                 | 122                 | 8                                | 1559                             | 8                   | 20                               | -18  |  |

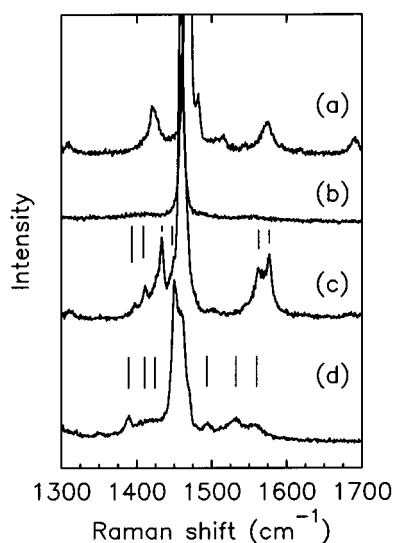


FIG. 5. Raman spectra between  $1300\text{ cm}^{-1}$  and  $1700\text{ cm}^{-1}$  of  $\text{C}_{60}$ ,  $\text{RbC}_{60}$  both at  $450\text{ K}$  [(a) and (b)], and pressure-polymerized  $\text{C}_{60}$  and  $\text{RbC}_{60}$  at room temperature [(c) and (d)].

former  $H_g$  modes into  $A_g$ ,  $B_{g1}$ ,  $B_{2g}$ , and  $B_{3g}$  and also new modes in the spectrum can be expected. A correlation table of the symmetry groups  $I_h$  and  $D_{2h}$  is shown in Table I.

The identical mode pattern for the orthorhombic phase as prepared from pressure polymerization and charge-transfer polymerization, respectively, is unexpected as the two routes of preparation are very different. As a consequence of the result we conclude that the overall crystal structure and the local structures are the same for the two polymers. The broad overlapping structures in the x-ray pattern indicate that the disorder is somewhat larger in the pressure-polymerized material. In this sense we can consider  $\text{RbC}_{60}$  as the doped form of the pressure-polymerized species. This view is further strongly supported by the very similar charge-induced line shifts between the pressure-polymerized material and the polymer obtained by cooling from the rocksalt phase. This similarity is immediately evident from a comparison between columns the eighth and ninth columns in Table II. The only exception is the mode  $H_g(1)$  where the average shift for the monomers is  $-3\text{ cm}^{-1}$  whereas for the polymers no shift is observed. This may have to do with a much smaller electron-phonon coupling for this mode in the polymer as compared to the same mode in the monomer. On the other hand the upshift of  $1\text{ cm}^{-1}$  for the total symmetric breathing mode at  $489\text{ cm}^{-1}$  [ $A_g(1)$ ] is exactly equal to the value for the monomer. It was explained in the latter as a Coulomb contribution to the force constants which yields an additional stiffening.<sup>19</sup> The overall shape of the breathing mode must therefore be retained in the polymer.

The splitting observed for the other total symmetric mode as a consequence of the transition to the polymeric state cannot be due to a reduction of symmetry on the molecule. It may be due to the geometrical arrangements of the chains in the lattice. The space group was determined at least for  $\text{RbC}_{60}$  as  $Pnmm$ ,<sup>6</sup> which means a primitive orthorhombic cell with two  $\text{C}_{60}$  molecules as a basis. This configuration allows for a Davidov splitting of nondegenerate modes. As

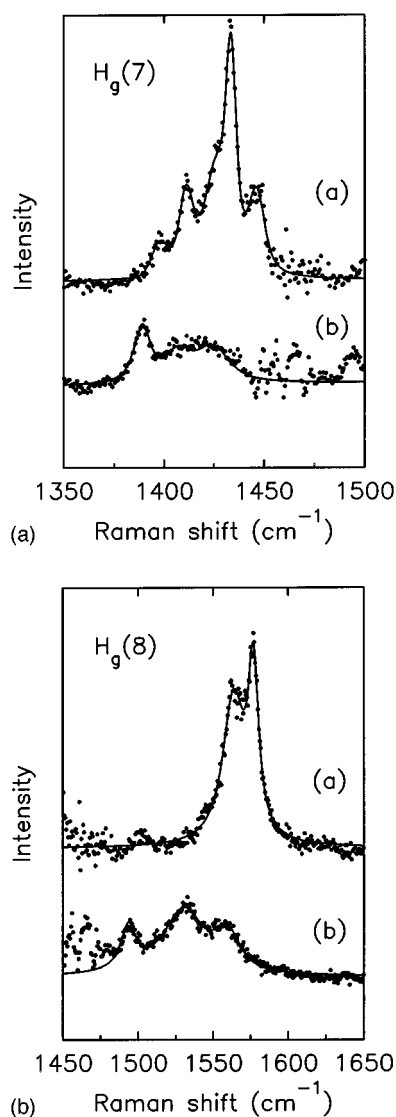


FIG. 6. Raman lines for the modes  $H_g(7)$  and  $H_g(8)$  for the two polymeric phases after subtraction of the overlapping contributions from the  $A_g(2)$  pinch mode.

the overall spectrum is so similar for the doped and the undoped polymer the Davidov splitting may also be the reason for the splitting in the latter.

The lack of the observation of interball modes in the present work may originate from the fact that these modes are very weak for linear chains. Using a Nd-YAG laser for excitation the intensities of these modes are approximately a factor 20 weaker than the intensities of the  $A_g(1)$  mode.<sup>15</sup> Assuming that the intensity ratio between the interball modes and the low-frequency  $\text{C}_{60}$  modes is more or less the same for the excitation with the two different lasers, the former can hardly be detected with a green laser excitation. The penetration depth and thus the scattering volume for the Nd-YAG laser are much larger than for the green laser.

The new mode at  $344\text{ cm}^{-1}$  is interesting. It is very well defined in both polymers but not observed in the monomers and not after photopolymerization.<sup>20</sup> It is obviously a very good fingerprint for a well defined extended chain. This mode was also found in theoretical calculations for the un-

doped chain<sup>21</sup> but not for the dimers or trimers.<sup>22</sup> Considering it as the fifth component of the totally split  $H_g(1)$  mode is in agreement with recent results of Renker *et al.*<sup>23</sup>

A detailed inspection of the difference in linewidth between the undoped and the doped polymer is interesting. *A priori* the linewidths for the pressure-polymerized material may be expected to be larger as compared to that of the doped polymer since the latter was a single crystal. In spite of this the widths for almost all registered lines are broader for the doped polymer. As the latter is a metal the increased linewidths may have to do with a coupling of the vibrations to free carriers as is well known for the phases  $K_3C_{60}$  and  $Rb_3C_{60}$ . The effect of broadening is, however, too small to be evaluated even qualitatively. This holds at least for the  $H_g$  modes up to  $H_g(6)$ . For  $H_g(7)$  and  $H_g(8)$  it is different, as can be seen already from Fig. 5. The strong broadening of the modes for the metallic material is more convincingly demonstrated if the overlap with the perturbing wings from the  $A_g(2)$  mode is subtracted. The result is shown in Fig. 6 for the two polymers. The derived increase in linewidths is about a factor 2 for the  $H_g(8)$  and slightly less for the  $H_g(7)$ . From the experience with the classical metallic phases of the alkali- $C_{60}$  family it is well justified to interpret this broadening as a coupling to free carriers. The observed broadening is, however, still a factor 3 smaller than the broadening for the corresponding  $H_g$  modes in  $K_3C_{60}$ . For a comparison the electron-phonon coupling constants of  $H_g(7)$  and  $H_g(8)$  were calculated for  $K_3C_{60}$  and  $RbC_{60}$  using Allen's formula. (Note: The formula used here is different by a factor of 4 from various previous reports.<sup>24,25</sup> Following the results of (Refs. 26 and 27) the version used here is the correct one.) Because of the different values for the density of states at the Fermi level we rather determine the product of the coupling constants with the density of states:

$$\lambda_i N(E_F) = g_i \frac{\gamma_i}{2\pi \omega_i^2}. \quad (1)$$

$\lambda N(E_F)$  for the  $H_g(7)$  and  $H_g(8)$  were found to be 0.145 and 0.109 in  $K_3C_{60}$  (Ref. 24) whereas the results for orthorhombic  $RbC_{60}$  are only 0.032 and 0.067.

As the broadening for the lower-frequency  $H_g$ -derived modes is even less in the polymeric material we conclude that the total electron-phonon coupling is much smaller in the polymeric metal as compared to the monomeric metal. This explains why so far no superconductivity was observed for the polymeric  $AC_{60}$  phase. In this sense it supports a speculation of Janossy *et al.*<sup>28</sup> about the strong difference in the spin lattice relaxation rates between  $Rb_3C_{60}$  and  $RbC_{60}$ . The observed difference was interpreted as a difference in the electron-phonon coupling for the two systems. Because of the weak coupling  $RbC_{60}$  and  $CsC_{60}$  rather undergo a magnetic ordering transition to an insulating state on cooling and  $KC_{60}$  remains metallic to the lowest temperatures observed so far.

## V. CONCLUSIONS

Summarizing, our measurements have shown that pressure-polymerized  $C_{60}$  and  $RbC_{60}$  have a nearly identical Raman spectrum with respect to mode positions and line splitting. We conclude from this result that both materials have the same orthorhombic structure and form linear chains. From a comparison of the mode positions the effect of the charge transfer could be determined. Line broadening of the high-frequency modes in the doped compound compared with the modes in pressure-polymerized  $C_{60}$  is consistent with the metallic behavior of the  $AC_{60}$  compound but the electron-phonon coupling constants are much weaker.

## ACKNOWLEDGMENTS

We acknowledge M. Haluška for supporting us with single crystals and the Hoechst AG for the  $C_{60}$  raw material. We are also grateful for valuable discussions with O. Gunnarsson and B. Burger. The work was supported by the FWF in Austria, Project No. P09741, and the research grant from The Swedish National Research Council (NFR) in Sweden.

<sup>1</sup>A.M. Rao, P. Zhou, K.-A. Wang, G.T. Hager, J.M. Holden, Y. Wang, W.-T. Lee, X.-X. Bi, P.C. Eklund, D.S. Cornett, M.A. Duncan, and I.J. Amster, *Science* **259**, 955 (1993).

<sup>2</sup>J. Winter and H. Kuzmany, *Solid State Commun.* **84**, 935 (1992).

<sup>3</sup>D.M. Poirier and J.H. Weaver, *Phys. Rev. B* **47**, 10 959 (1993).

<sup>4</sup>Q. Zhu, O. Zhu, N. Bykovetz, J.E. Fisher, A.R. McGhie, W.J. Romanow, C.L. Lin, R.M. Strongin, M.A. Cichy, and A.B. Smith III, *Phys. Rev. B* **47**, 13 948 (1993).

<sup>5</sup>S. Pekker, A. Janossy, L. Mihaly, O. Chauvet, M. Carrard, and L. Forro, *Science* **265**, 1077 (1994).

<sup>6</sup>P. Stephens, G. Bortel, G. Faigel, M. Tegze, A. Janossy, S. Pekker, G. Oszlanyi, and L. Forro, *Nature (London)* **370**, 636 (1994).

<sup>7</sup>O. Chauvet, G. Oszlanyi, L. Forro, P.W. Stephens, M. Tegze, G. Faigel, and A. Janossy, *Phys. Rev. Lett.* **72**, 2721 (1994).

<sup>8</sup>R. Winkler, T. Pichler, and H. Kuzmany, *Appl. Phys. Lett.* **66**, 1211 (1995).

<sup>9</sup>F. Bommeli, L. Degiorgi, P. Wachter, Ö. Legeza, A. Janossy, G. Oszlanyi, O. Chauvet, and L. Forro, *Phys. Rev. B* **51**, 14 794 (1995).

<sup>10</sup>Y. Iwasa, T. Arima, R.M. Fleming, T. Siegrist, O. Zhou, R.C. Haddon, L.J. Rothberg, K.B. Lyons, H.L. Carter, Jr., A.F. Hebard, R. Tycko, G. Dabbagh, J.J. Krajewski, G.A. Thomas, and T. Yagi, *Science* **264**, 1570 (1994).

<sup>11</sup>M. Núñez Regueiro, L. Marques, J.-L. Hodeau, O. Béthoux, and M. Perroux, *Phys. Rev. Lett.* **74**, 278 (1995).

<sup>12</sup>M. Núñez Regueiro, P. Monceau, and J.-L. Hodeau, *Nature (London)* **355**, 237 (1992).

<sup>13</sup>V. Blank, M. Popov, S. Buga, V. Davydov, V.N. Denisov, A.N. Ivlev, B.N. Mavrin, V. Agafonov, R. Ceolin, H. Szwarc, and A. Rassat, *Phys. Lett. A* **188**, 281 (1994).

<sup>14</sup>P.-A. Persson, U. Edlund, P. Jacobsson, D. Johnels, A. Soldatov, and B. Sundqvist, *Chem. Phys. Lett.* **258**, 540 (1996).

<sup>15</sup>A. Soldatov, P. Jacobsson, P.-A. Persson, B. Sundqvist, U. Edlund, and D. Johnels, in *Proceedings of the International Winterschool on Electronic Properties of Novel Materials (IWEPNM 96), Kirchberg, Austria*, edited by H. Kuzmany *et al.* (World Scientific, Singapore, 1996), p. 344.

<sup>16</sup>B. Sundqvist, O. Anderson, U. Edlund, A. Fransson, A. Inaba, P. Jacobsson, D. Johnels, P. Launois, C. Meingast, R. Moret, T.

- Moritz, P.-A. Persson, A. Soldatov, and T. Wagberg, *Recent Advances in the Chemistry and Physics of Fullerenes and Related Materials*, Proceedings of the 189th ECS Meeting, Symposium on Fullerenes: Chemistry, Physics, and New Directions VIII, Los Angeles, 1996, edited by R. S. Ruoff and K. M. Kadish (ECS, Pennington, 1996), Vol. 3, p. 1014–1028.
- <sup>17</sup>J. Winter and H. Kuzmany, *Phys. Rev. B* **52**, 7115 (1995).
- <sup>18</sup>J. Winter and H. Kuzmany, *J. Raman Spectrosc.* **27**, 373 (1996).
- <sup>19</sup>R.A. Jishi, R.M. Mirie, and M.S. Dresselhaus, *Phys. Rev. B* **45**, 13 685 (1992).
- <sup>20</sup>B. Burger, J. Winter, and H. Kuzmany (unpublished).
- <sup>21</sup>G.B. Adams, J.B. Page, O.F. Sankey, and M. O’Keeffe, *Phys. Rev. B* **50**, 17 471 (1994).
- <sup>22</sup>D. Porezag, M.R. Pederson, T. Frauenheim, and T. Köhler, *Phys. Rev. B* **52**, 14 963 (1995).
- <sup>23</sup>B. Renker, R. Heid, F. Gompf, and H. Schober, in *Proceedings of the International Winterschool on Electronic Properties of Novel Materials (IWEPNM 96)*, Kirchberg, Austria, edited by H. Kuzmany *et al.* (World Scientific, Singapore, 1996), p. 136.
- <sup>24</sup>J. Winter and H. Kuzmany, *Phys. Rev. B* **53**, 655 (1996).
- <sup>25</sup>M.G. Mitch and J.S. Lannin, *J. Phys. Chem. Solids* **54**, 1801 (1993).
- <sup>26</sup>P.B. Allen, *Solid State Commun.* **14**, 937 (1974).
- <sup>27</sup>O. Gunnarsson (unpublished).
- <sup>28</sup>A. Janossy, O. Chauvet, J.R. Pekker, S. Cooper, and L. Forro, *Phys. Rev. Lett.* **71**, 1091 (1993).